

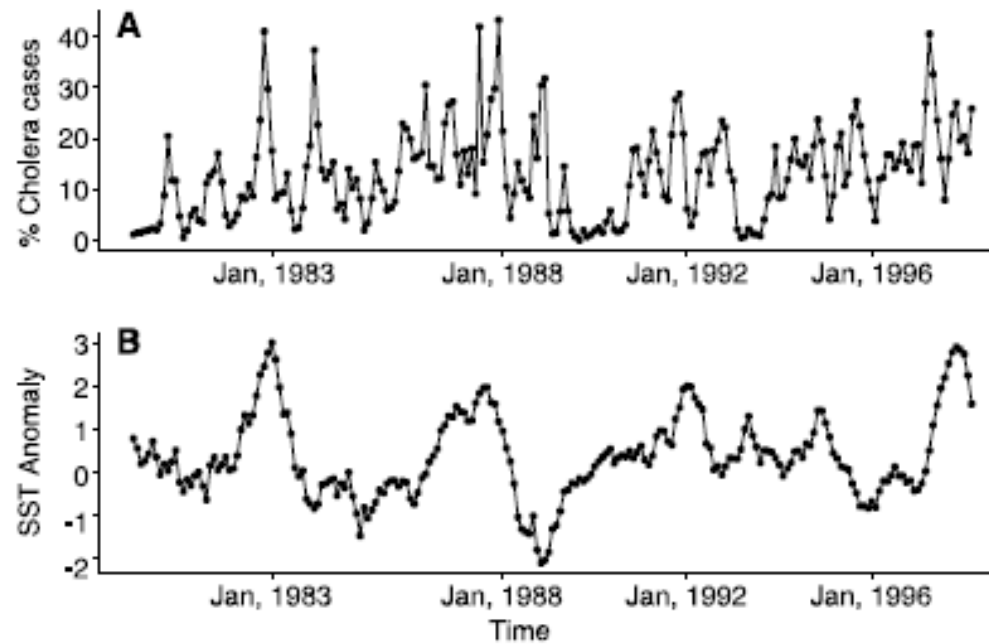
全球・南アジア・
バングラデシュの
気象水文環境変動と
ダッカの下痢症

寺尾 徹(香川大学教育学部)・林泰一・

A. S. G. Faruque・我妻ゆき子

コレラ患者と El Nino

- ◎ Dhakaのコレラ患者数
- ◎ El Nino(東太平洋の海面水温変動)

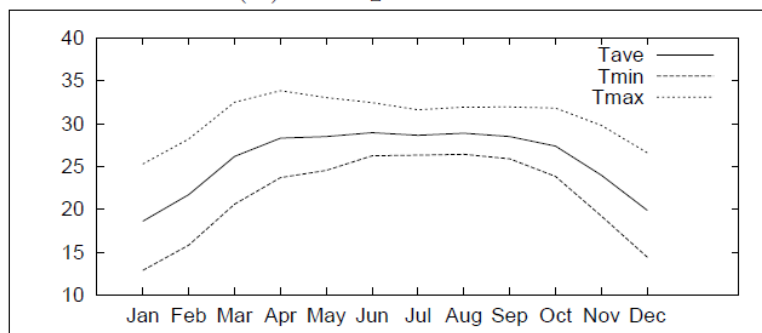


Rodo et al (2000)

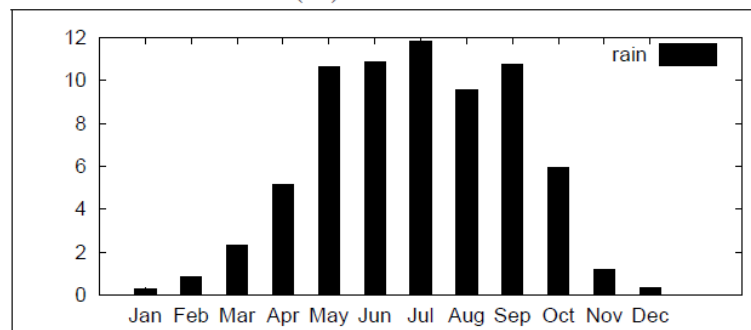
Dhakaの気象要素の季節変化

- ◎ 雨季と乾季
- ◎ プレモンスーンとモンスーン

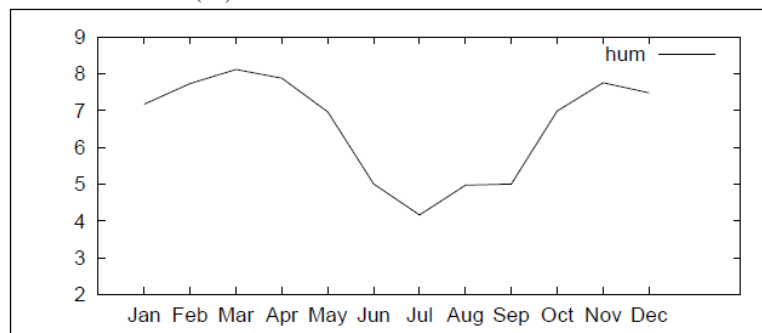
(a) Temperatures



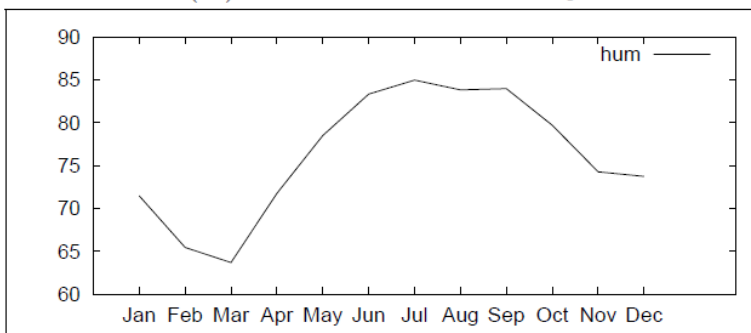
(b) Rainfall



(c) Sunshine Duration



(d) Relative Humidity

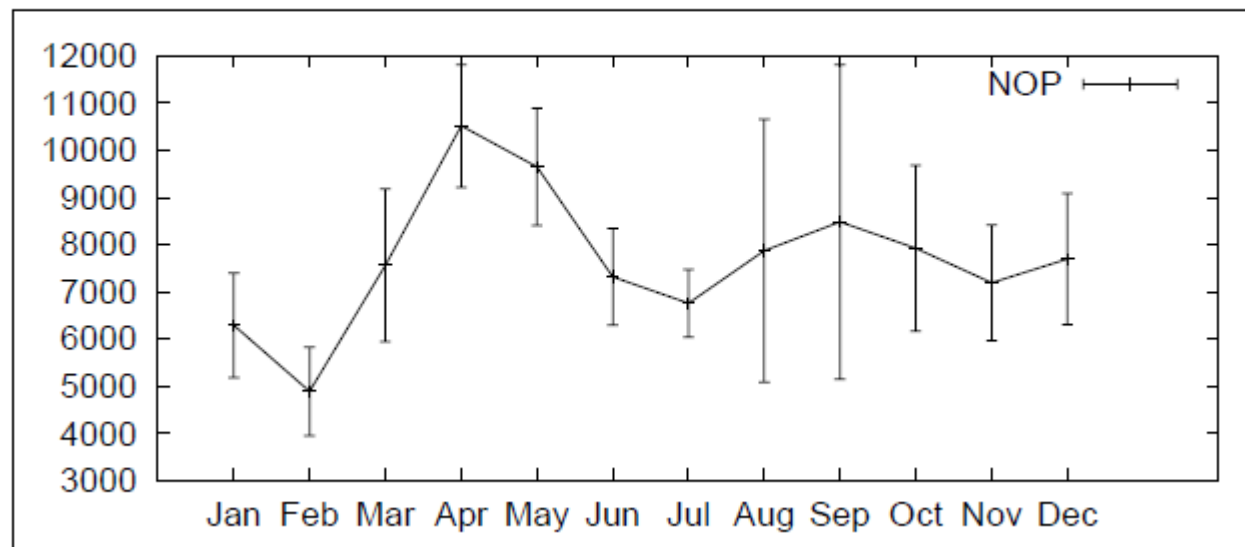


Dhaka患者数の季節変化

◎ Two peaks

- Hot Summer Peak (Apr-May)
- Late Rainy Season Peak (Aug-Oct)
 - Large interannual variability

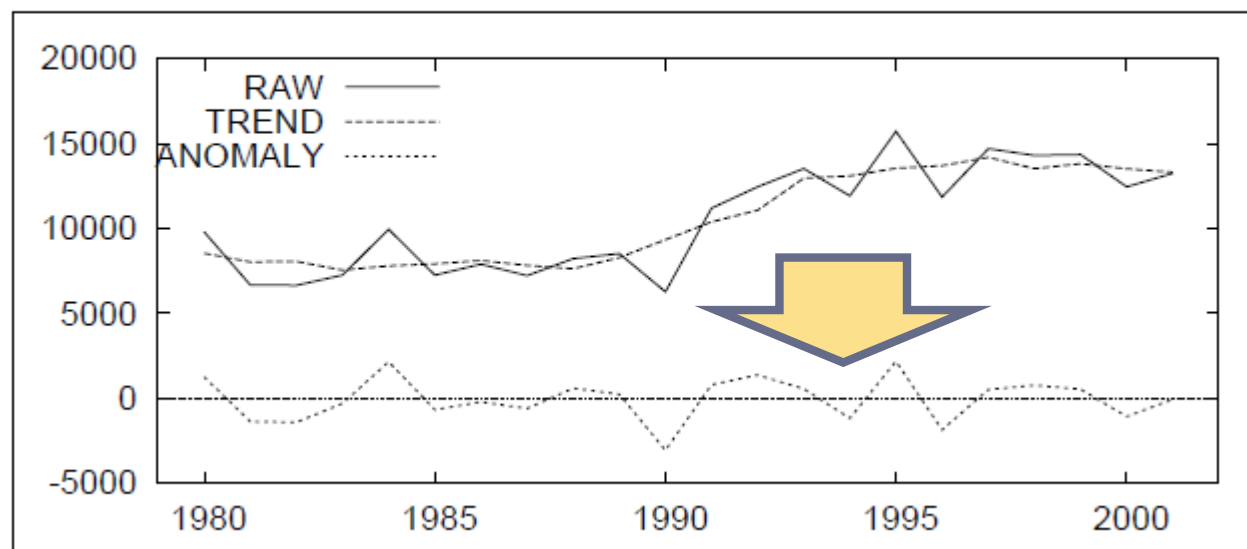
Number of Patients



患者数の年々変動の解析

- ◎ 生のデータには経年変動が入っている
 - 環境要因と関係のない社会的変動含む/線形でない
- ◎ 長いタイムスケールの変動(Trend)を除く
 - Trend: 5年間移動平均で定義

Number of Patients

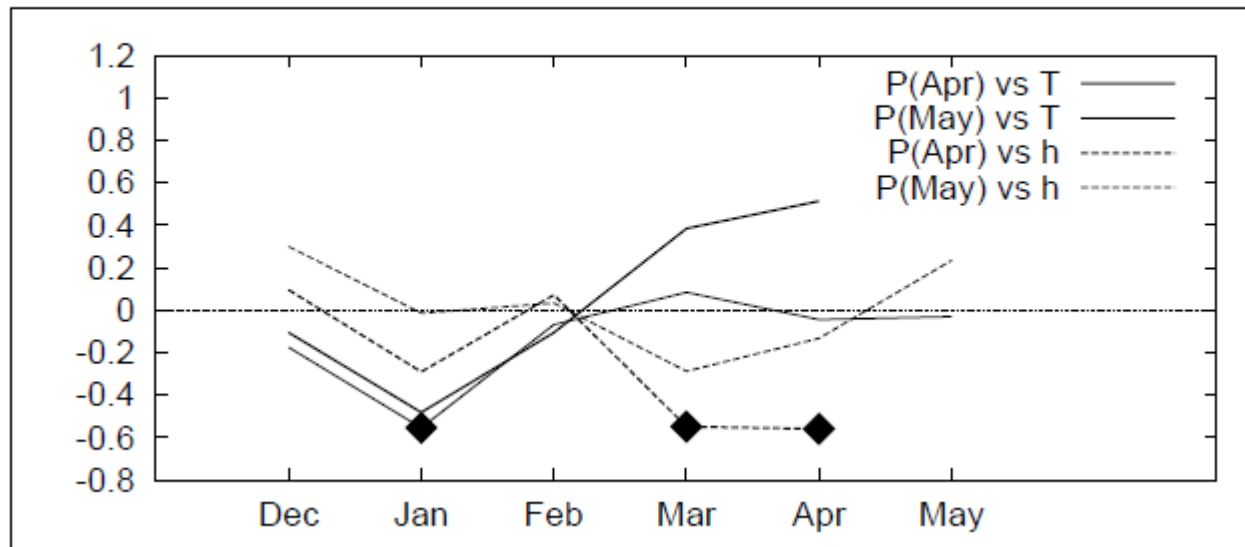


有意な相関なし

「春」の患者数と環境要因

- ◎ 4月: 3・4月の相対湿度と負の相関(99%有意)
- ◎ 5月: 1月の気温と負の相関(99%有意)
- ◎ 4月患者数 vs 5月患者数: 0.60(99%有意)

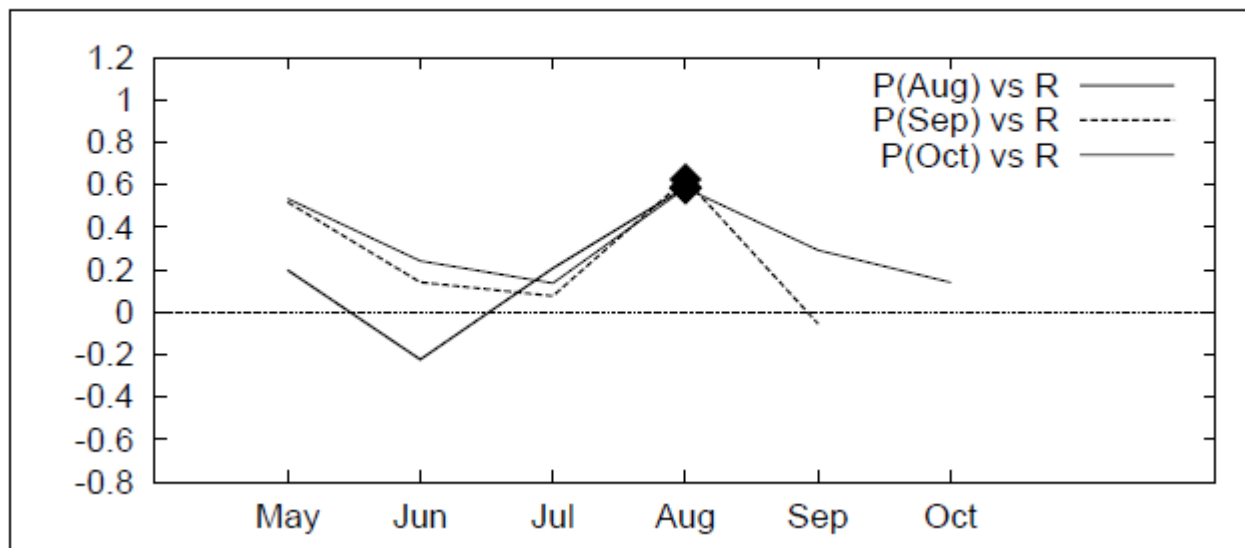
Correlation Coef.



「夏」の患者数と環境要因

- ◎ 8月・9月・10月患者数ともに、8月の雨量と正の相関(99%有意)
 - 雨が多い→水の汚染→患者の増加？

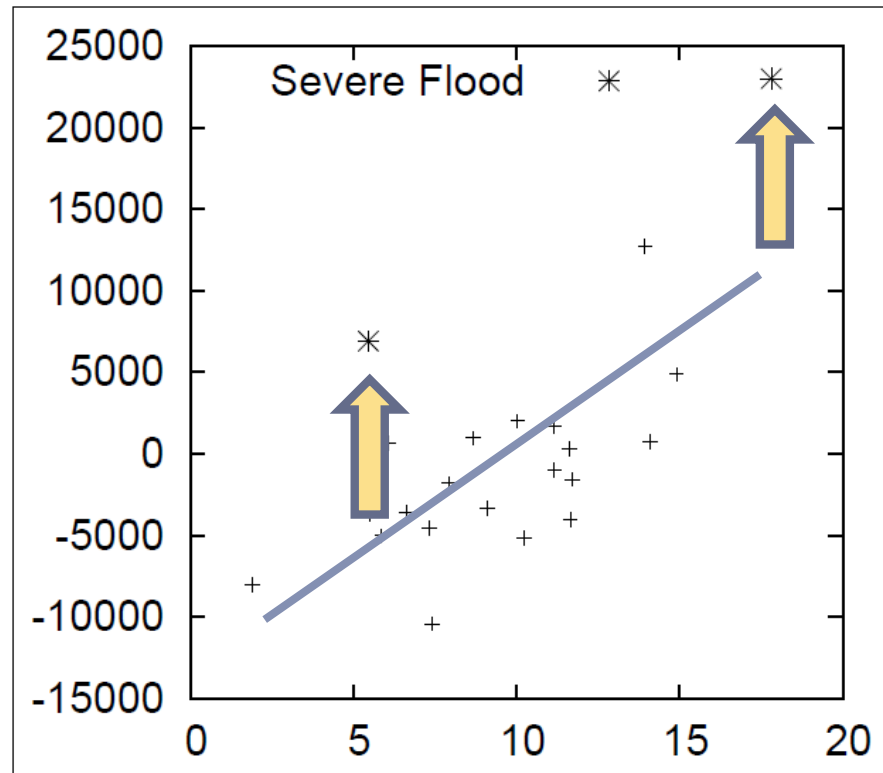
Correlation Coef.



大洪水と患者数の増加

- ◎ 大洪水の年は患者数が増える
 - BWDB:50%以上
- ◎ 大洪水がなくとも降水量と患者数は99%有意な正の相関を持つ

Scattered Diagram



8月の洪水と領域水循環過程

- ◎ 8月のDhakaの雨量を、入手可能な南アジアの降水・河川水の動向に位置づけ直す
- ◎ 6月から10月の右のパラメータの変化に対する因子分析
- ◎ Dhaka雨量
- ◎ 北東インド雨量
 - India Meteor. Dept.
- ◎ 河川流量
 - BWDB
 - Brahamputra+
 - Ganges

水循環の主要素と患者数

NEIS_Hと命名

◎ 第1因子

- インド北東部とバングラデシュの8月の雨
- バングラデシュへの8・9月の河川流量増大(雨よりも少し遅れる)

regional, 河川含む

◎ 第2因子

- バングラデシュの7月の雨
- インドの降水や河川とは関連しない

local, 雨のみ

「夏」の患者数と強い相関

factor	1	2
R_I		
Jun.		
Jul.	0.31	0.36
Aug.	0.99	-0.14
Sep.	-0.16	0.30
Oct.		
d		
Jun.		-0.13
Jul.	0.32	0.32
Aug.	0.79	
Sep.	0.69	0.10
Oct.	-0.11	-0.22
R		
Jun.	0.16	
Jul.		1.11
Aug.	0.56	
Sep.	-0.24	0.53
Oct.		-0.27
variance	0.182	0.134
cor. vs $P(ASO)$	0.77	0.19

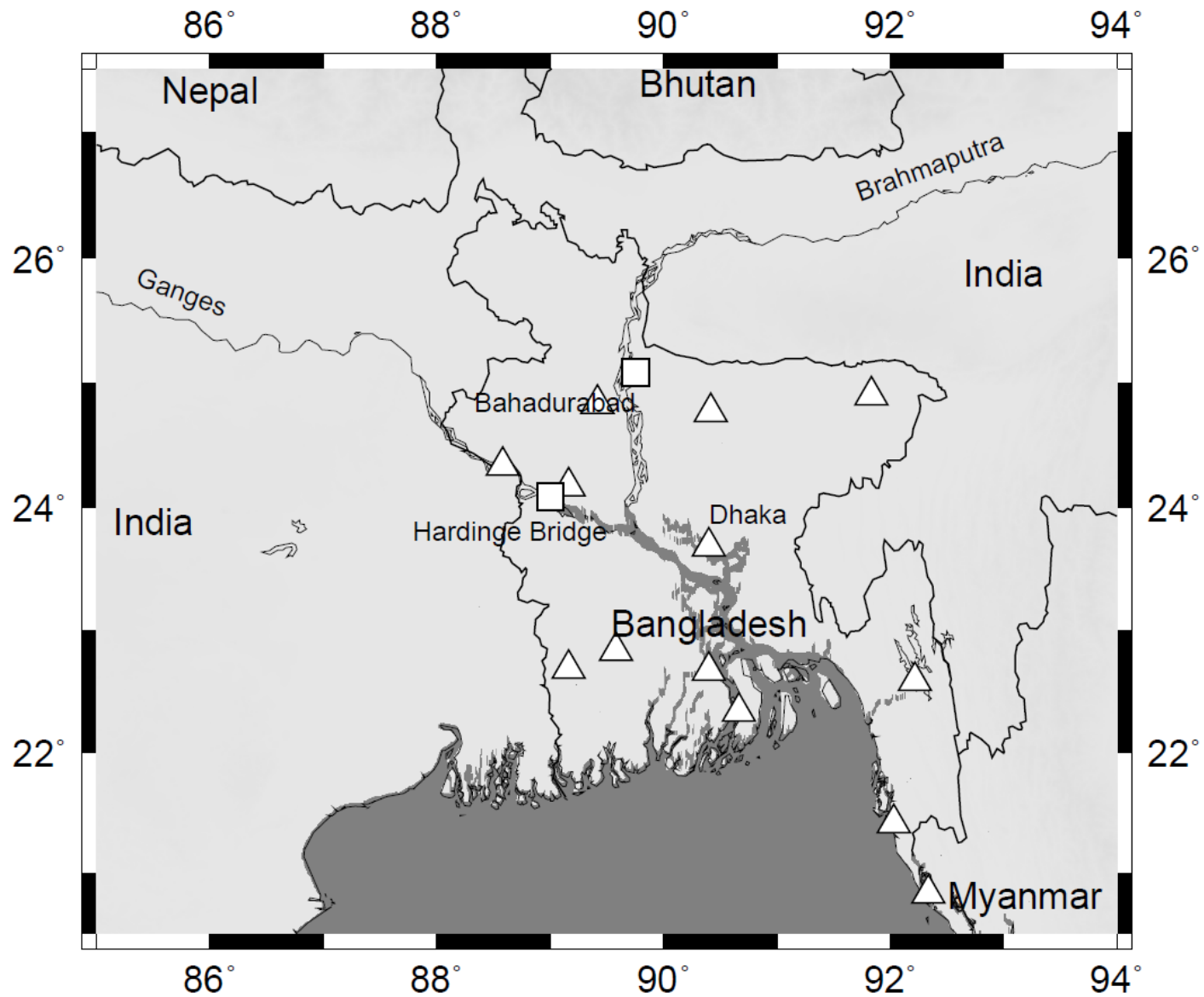


Figure 1: Map of northeastern Indian subcontinent. Triangles mark raingauges utilized in the present study. Boxes indicate observatories for river water discharge.

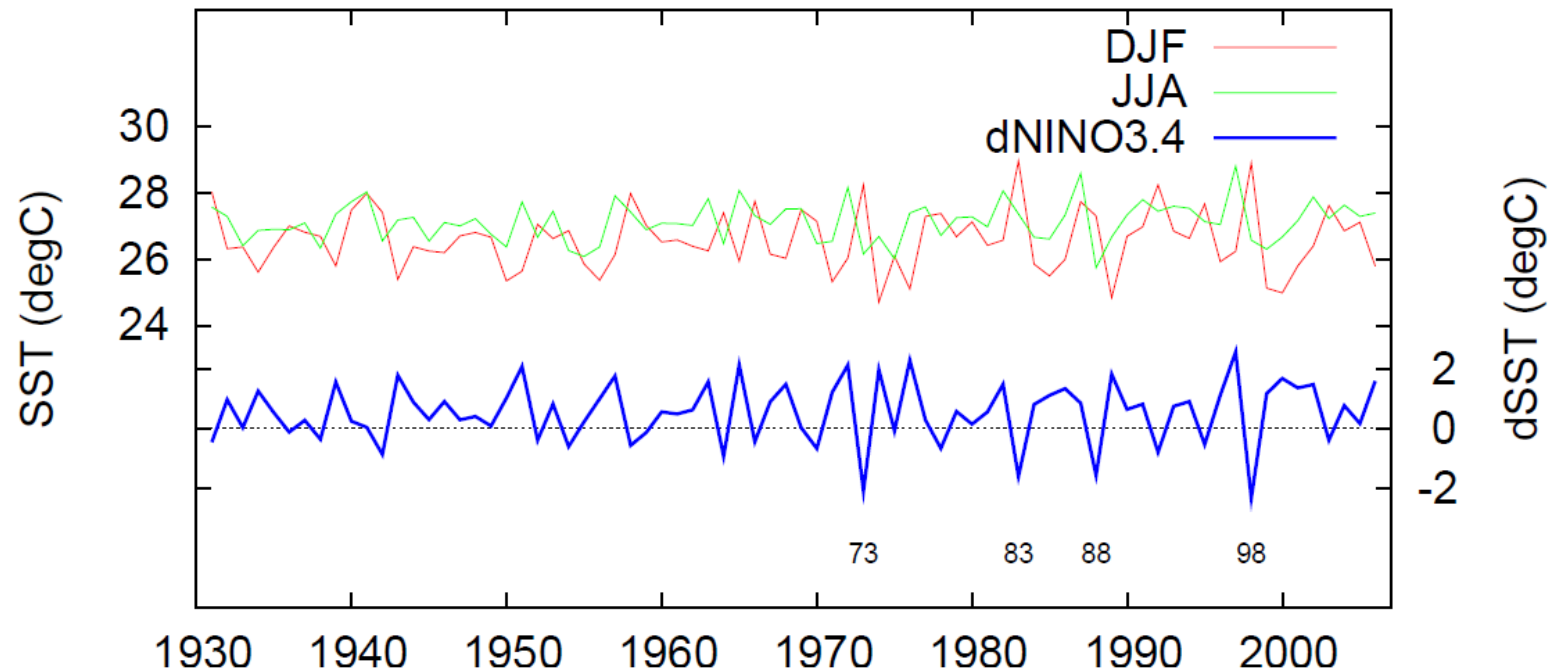


Figure 2: Interannual variation of SST averaged over NINO3.4 region for DJF (red line; previous December to February) and JJA (green line), whose values are given on the left axis in $^{\circ}\text{C}$. Difference between JJA and DJF, $d\text{NINO3.4}$, is blue line shown by right axis in $^{\circ}\text{C}$. Four rapid ENSO transition years between 1931 and 2006 are labeled by digits.

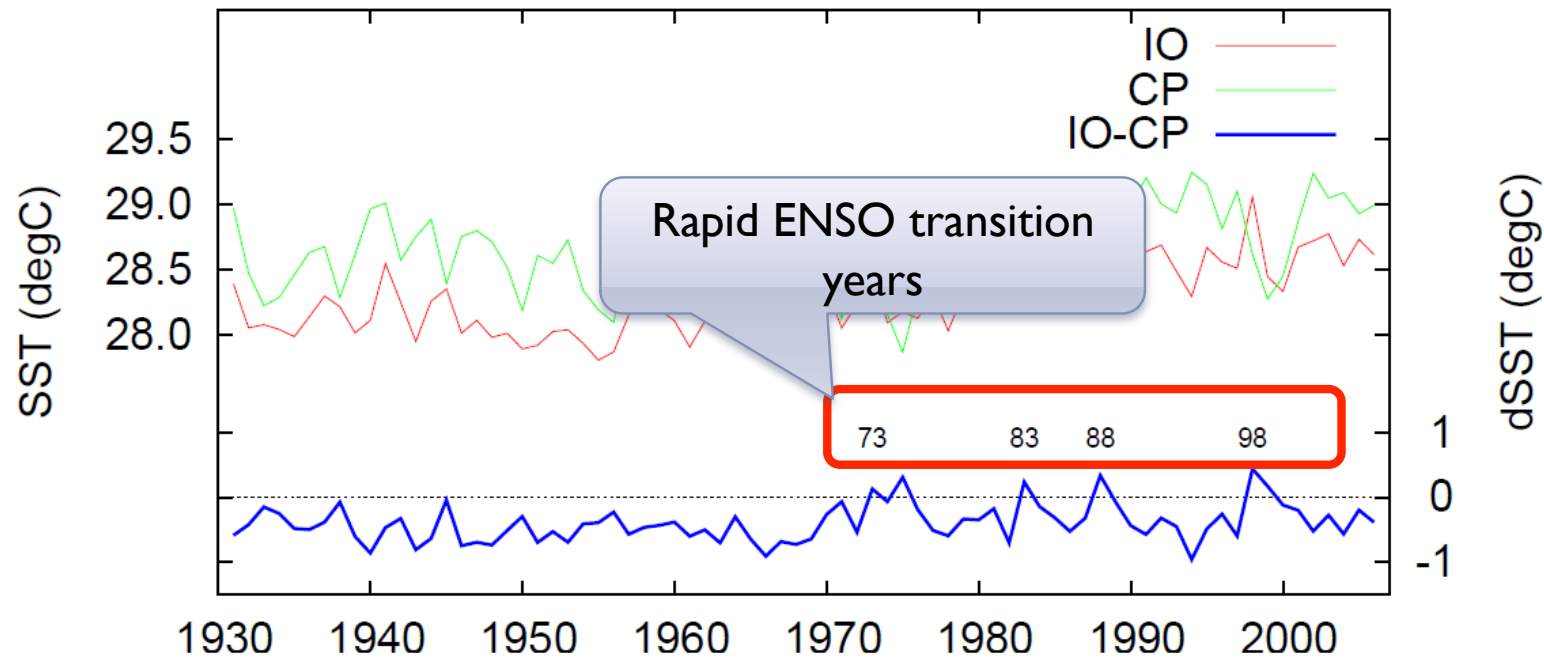


Figure 3: Interannual variation of JJA SST averaged over the equatorial Indian Ocean (red line, 10°S – 10°N , 60° – 120°E) and the central equatorial Pacific Ocean (green line, 10°S – 10°N , 150°E – 150°W), whose values are given on the left axis. Difference between the central Pacific and Indian Ocean (blue line, $d\text{SST}(\text{IO-CP})$), is shown by the right axis. The sample skewness of $d\text{SST}(\text{IO-CP})$ was 0.71. Four rapid ENSO transition years between 1931 and 2006 are labeled by digits.

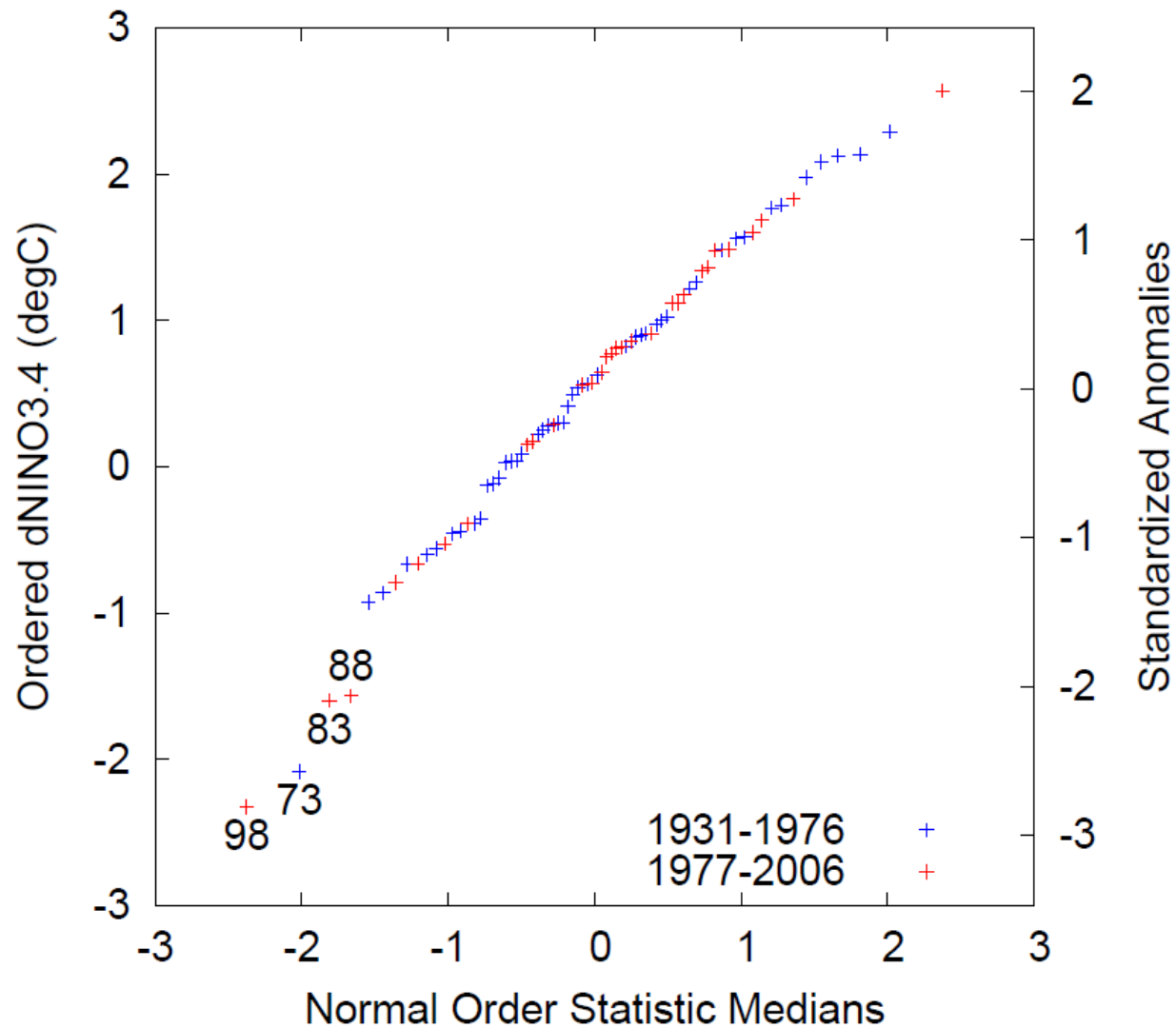
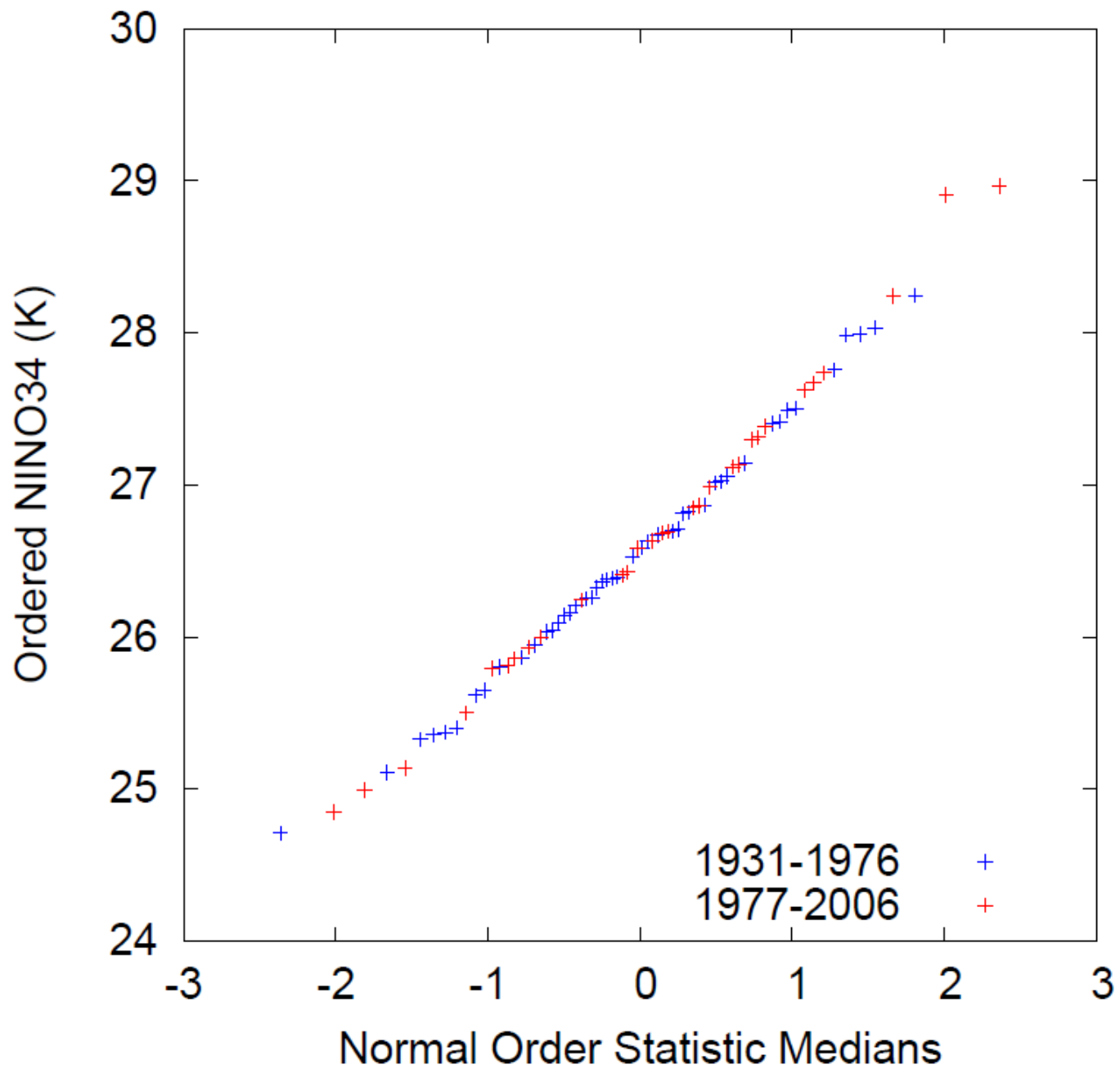
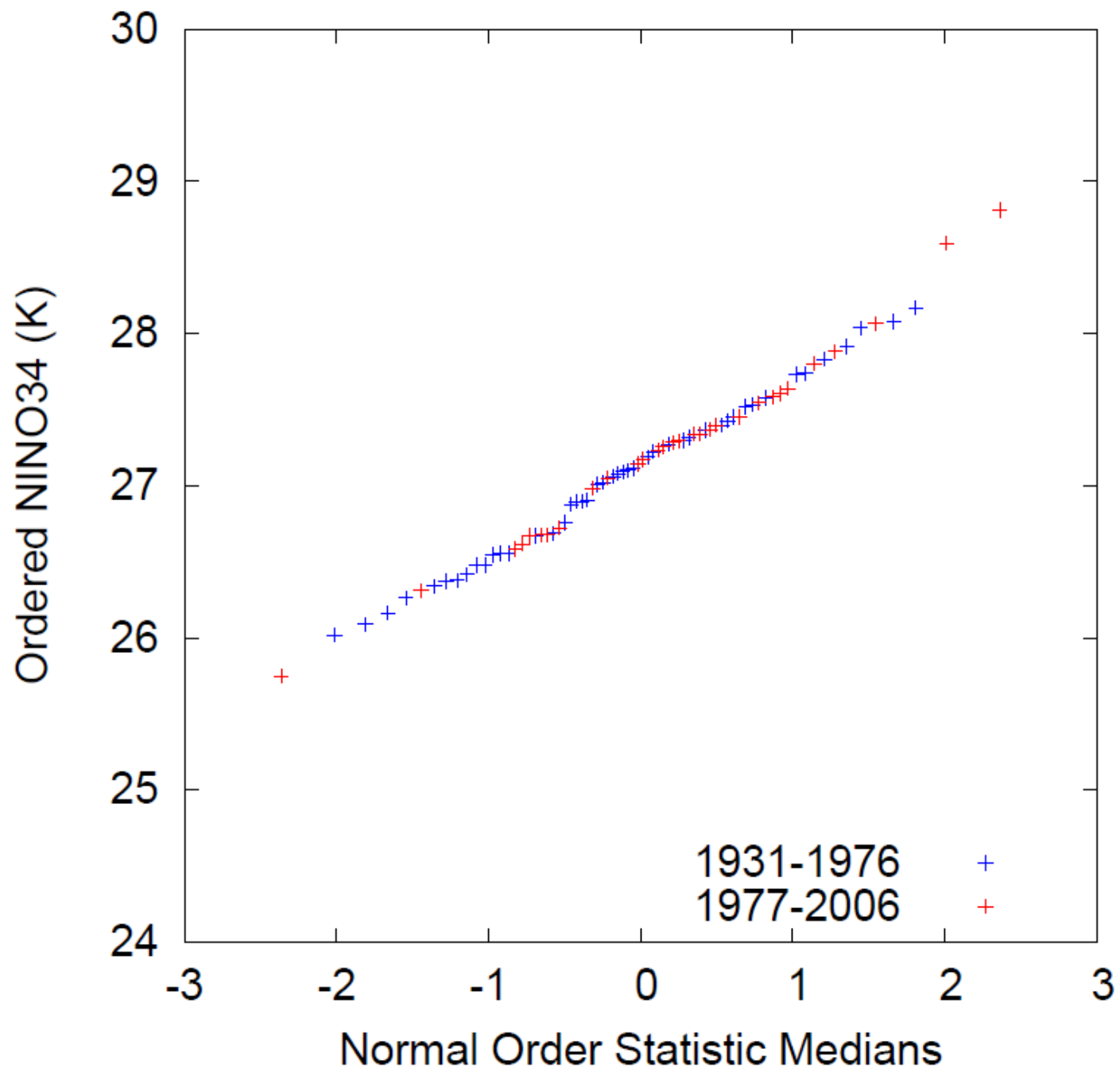


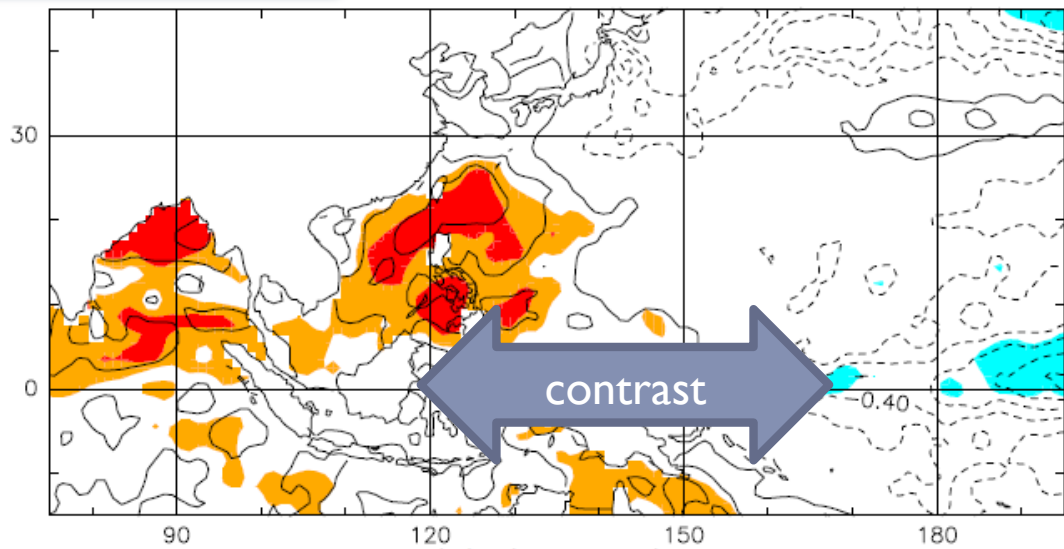
Figure S1: Normal probability plot for dNINO3.4 from 1931 to 2006. Vertical axes are the values of dNINO3.4 and its standardized anomaly, on the left side (in $^{\circ}\text{C}$) and the right side (dimensionless), respectively. Horizontal axis is the normal order statistic median (for $a = 1/3$ in Eq. 3.17 in Wilks (2006)). Four rapid ENSO transition years between 1931 and 2006 are labeled by digits. Data before and after the 1976/77 climate shift are shown by red and blue marks.



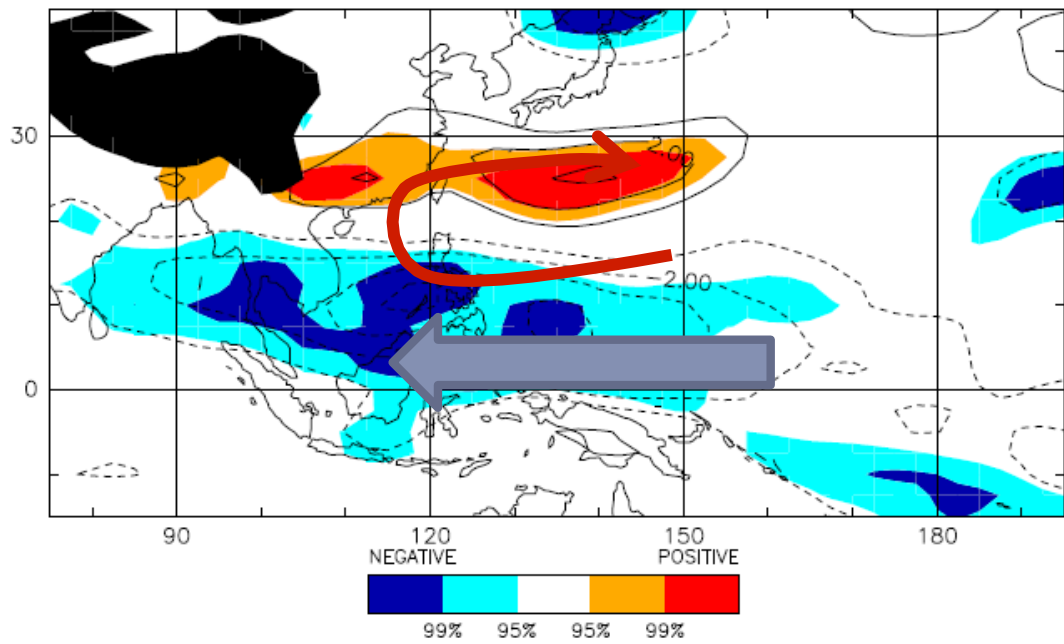


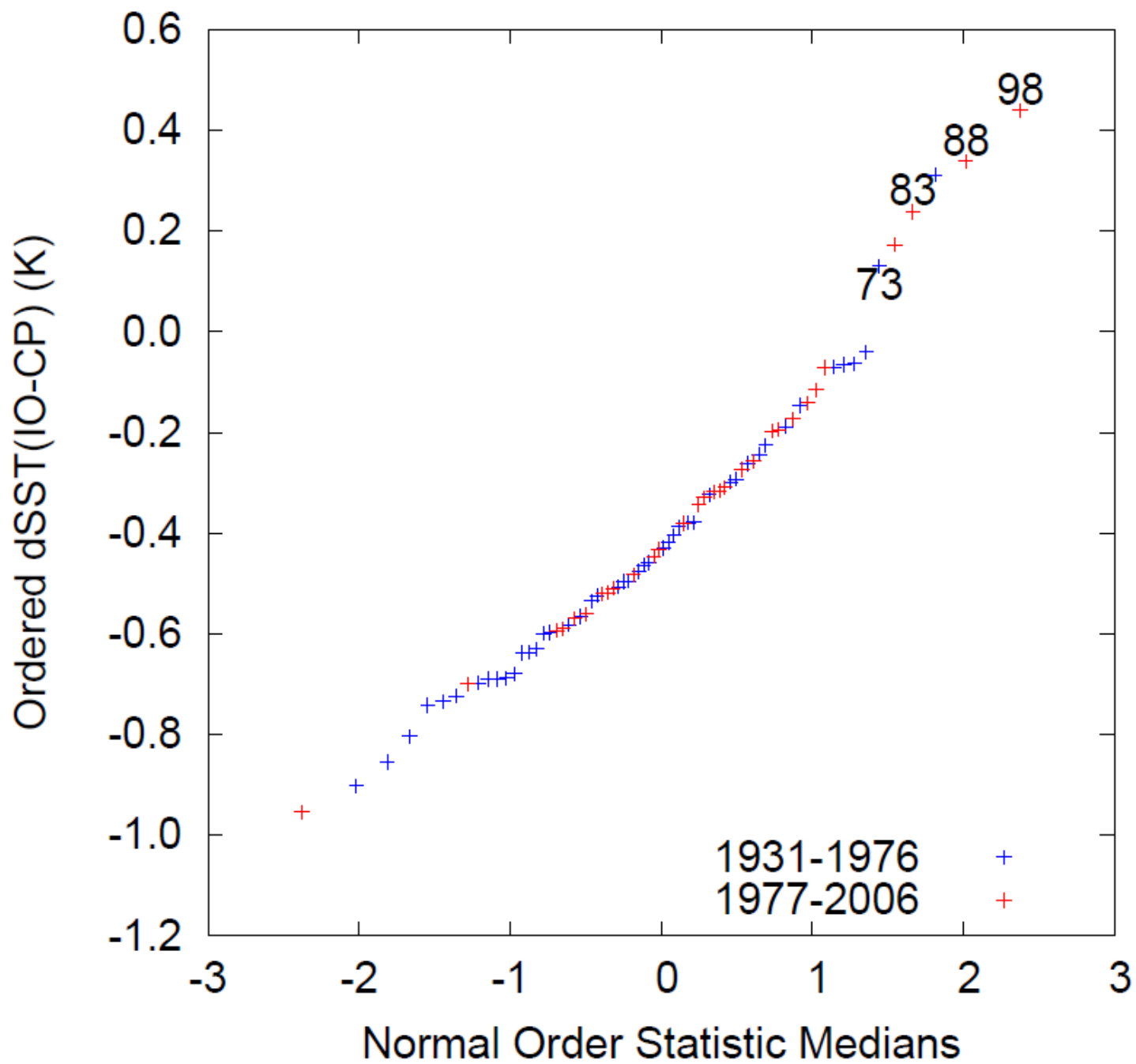
Rapid ENSO transition year

(a) SST



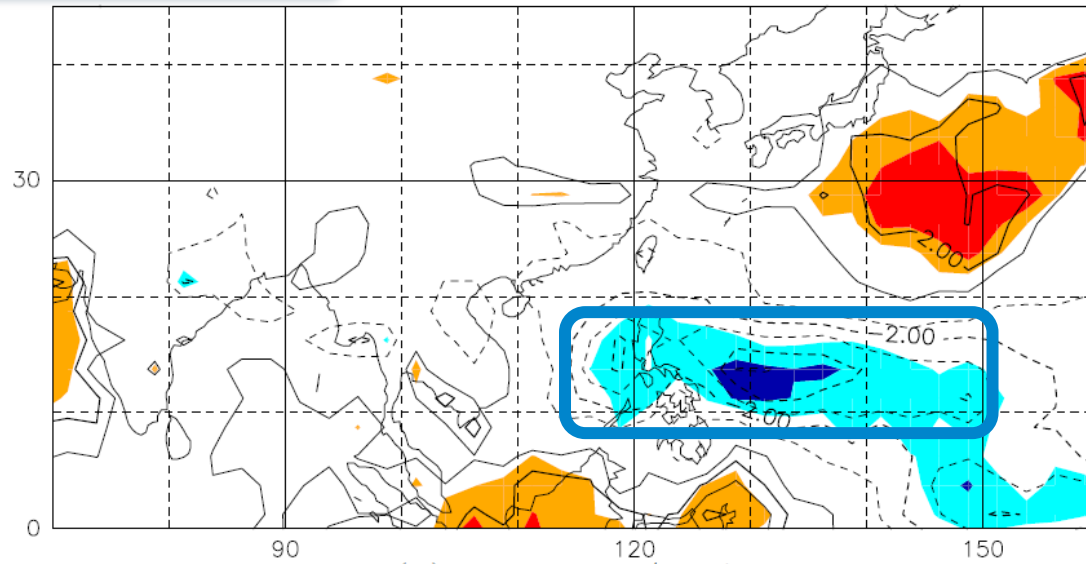
(b) $u(850 \text{ hPa})$





Rapid ENSO transition year

(a) CMAP / JJA



(b) Φ 850 hPa / JJA

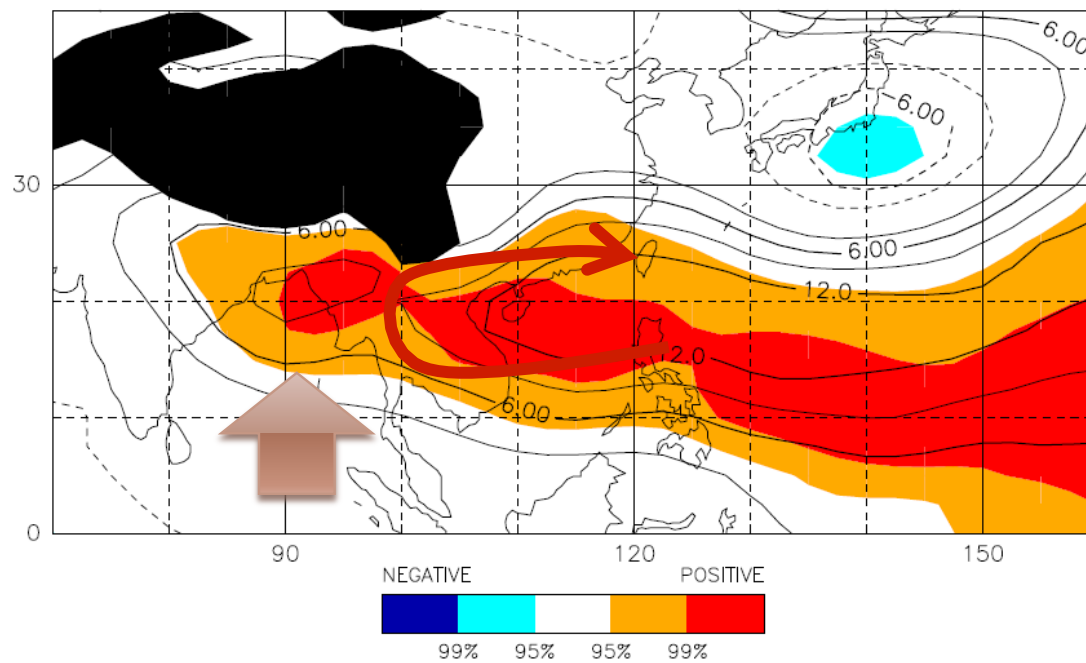
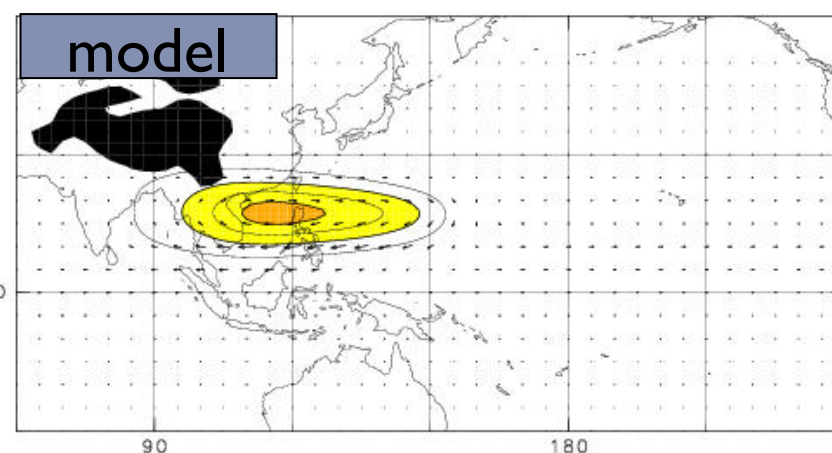
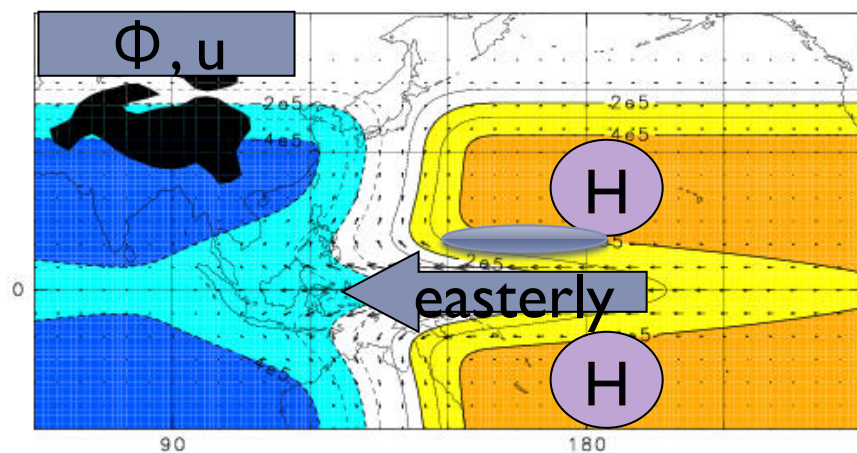
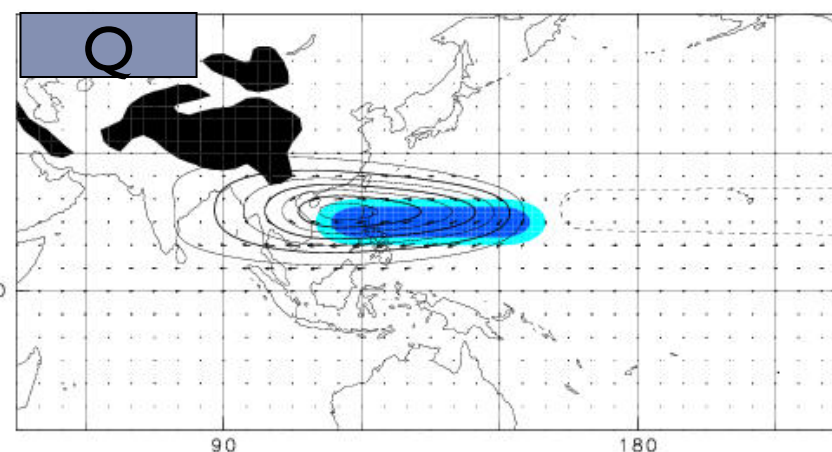
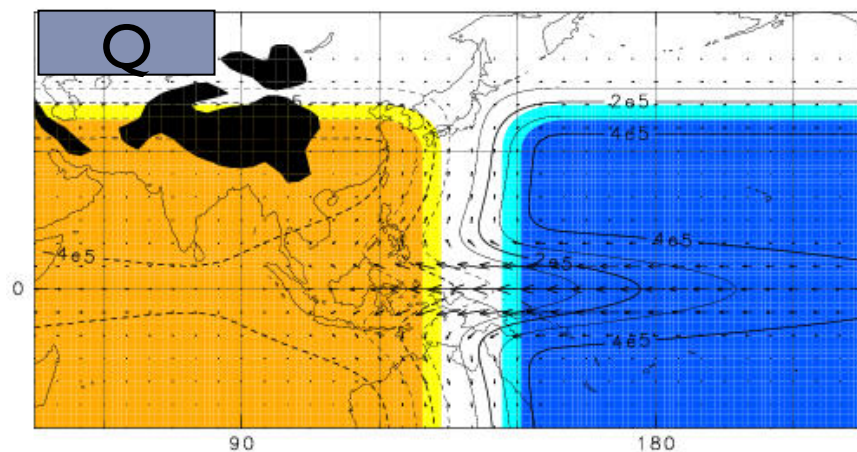


Figure 4. (a) Precipitation (Contour interval is 2 mm day⁻¹) and (b) 850 hPa

簡単モデルによる検討



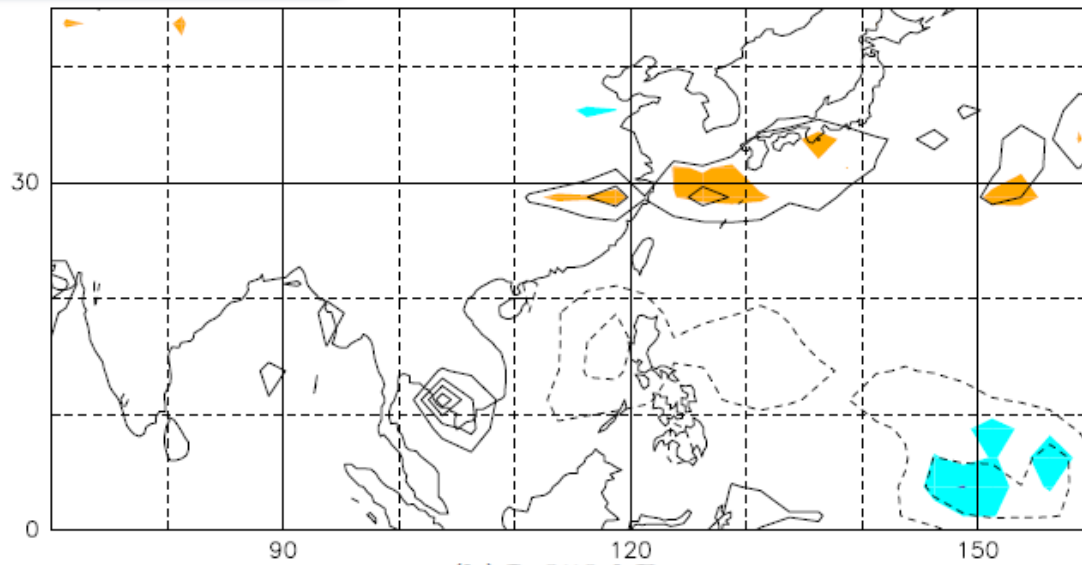
RAPID TRANSITION YEARの雨

Table 1: The Wilcoxon–Mann–Whitney rank-sum W in rapid ENSO transition years for parameters and indices associated with NEIM rainfall. Rank-sums significant at the 99% and 95% confidence levels in the Wilcoxon–Mann–Whitney test are indicated by bold and italic faces, respectively. As was defined in section 2, indices R_{NE} , R_{BP} , and D indicate the rainfall intensity for northeastern India, for Bengal Plain, the combined river water discharge of the Ganges and Brahmaputra rivers, and the monsoon Hadley index defined in Goswami et al. (1999), respectively.

index	n	Jun.	Jul.	Aug.	Sep.
R_{NE}	27	44	22	<i>15</i>	38
R_{BP}	27	53	34	12	63
D	19	31	30	21	10
MHI	27	61	26	6	<i>18</i>

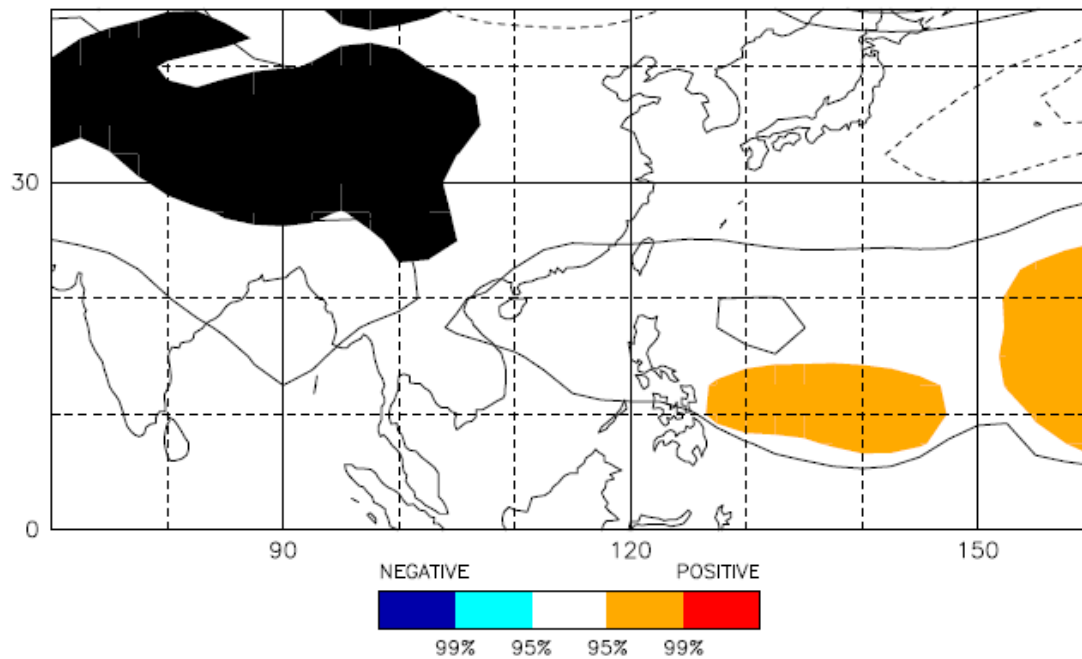
Rapid ENSO transition year

(a) CMAP



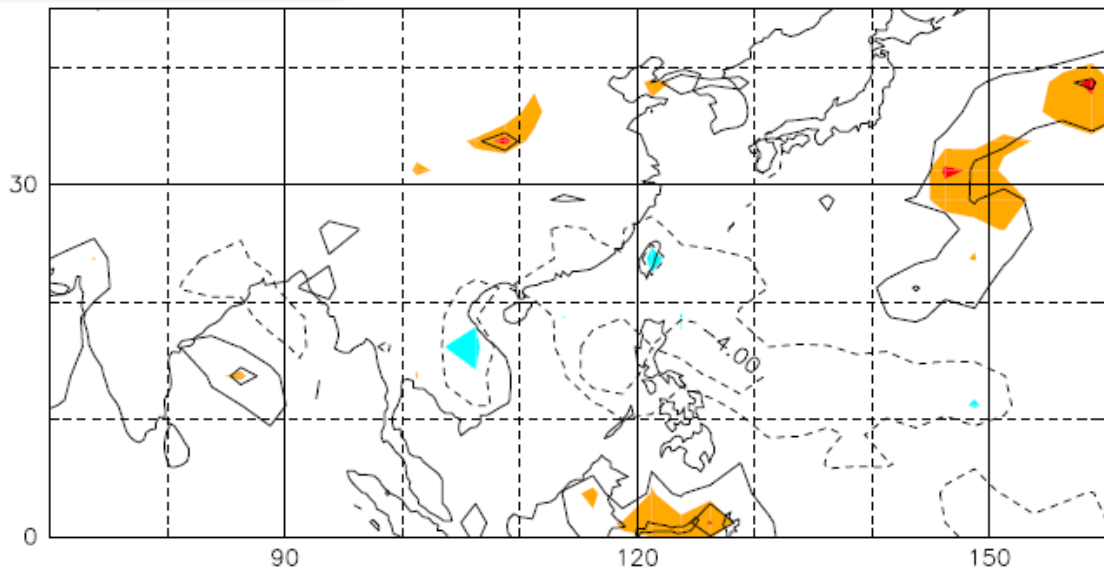
June

(b) Φ 850 hPa



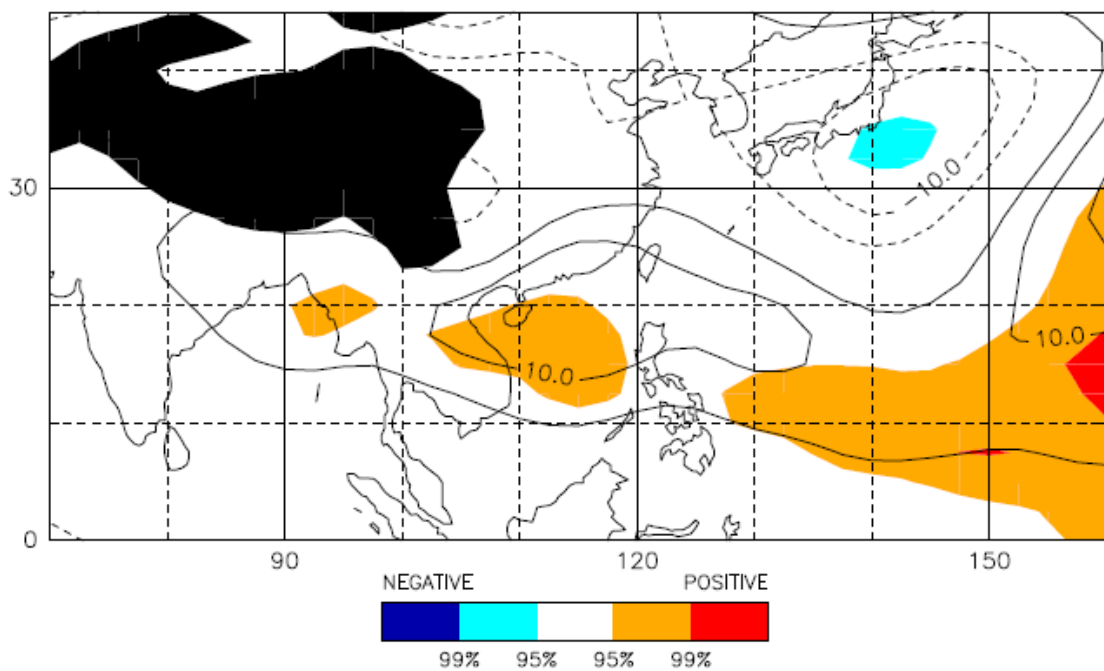
Rapid ENSO transition year

(a) CMAP



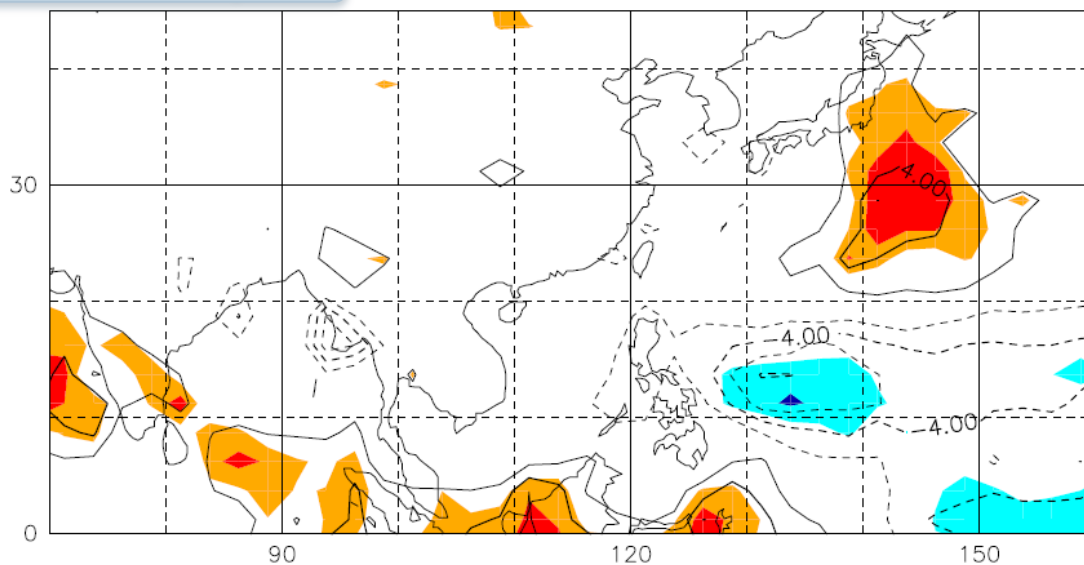
July

(b) Φ 850 hPa



Rapid ENSO transition year

(a) CMAP / August



August

(b) Φ 850 hPa / August

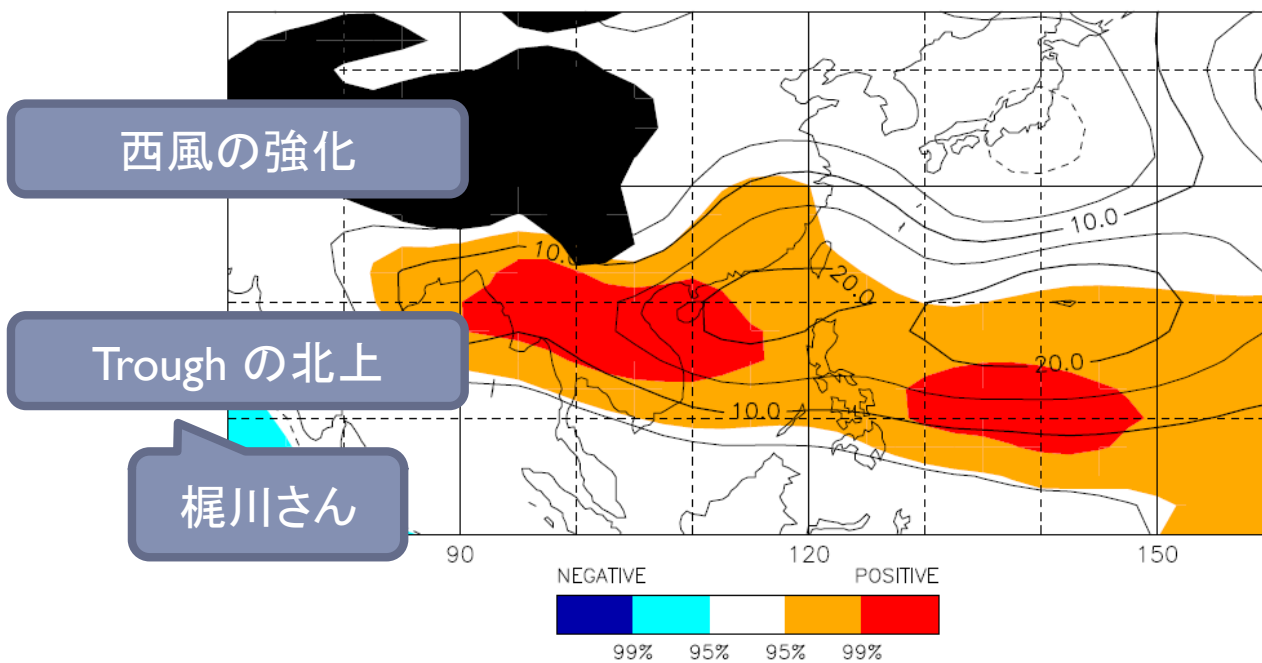
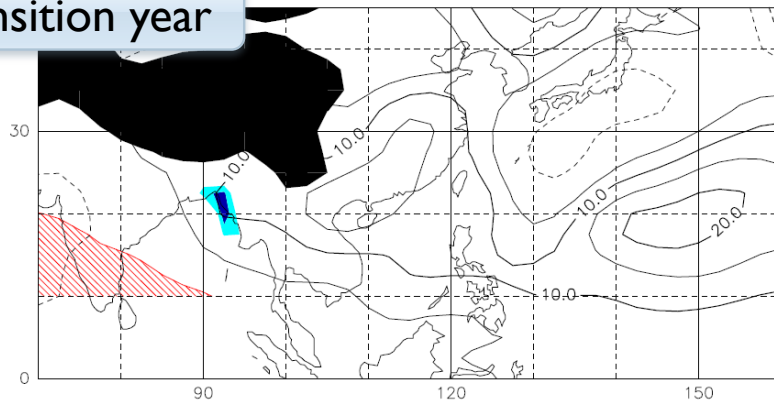


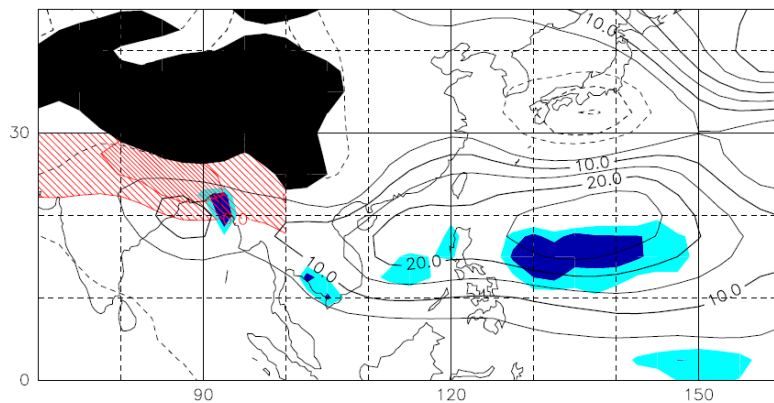
Figure 5: Same as Figure 4 except for August

Rapid ENSO transition year

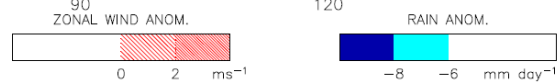
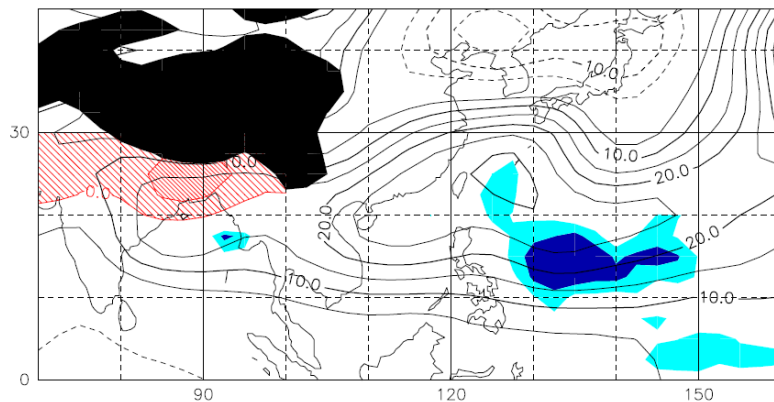
(a) August 1983



(b) August 1988



(c) August 1998

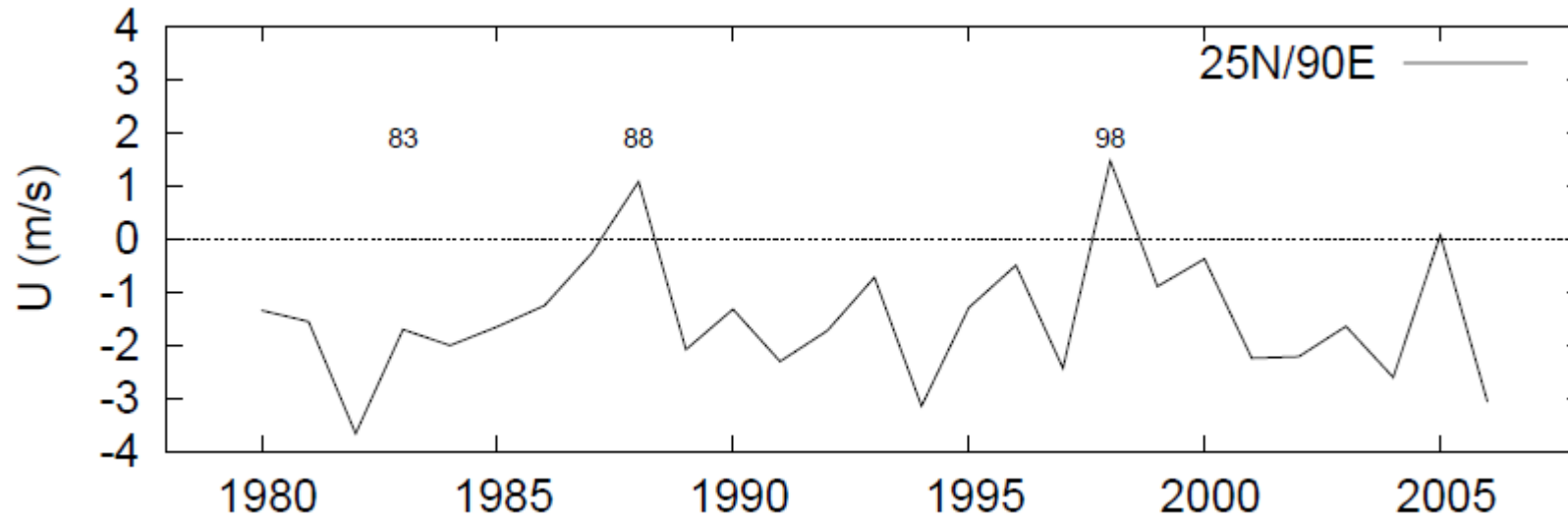


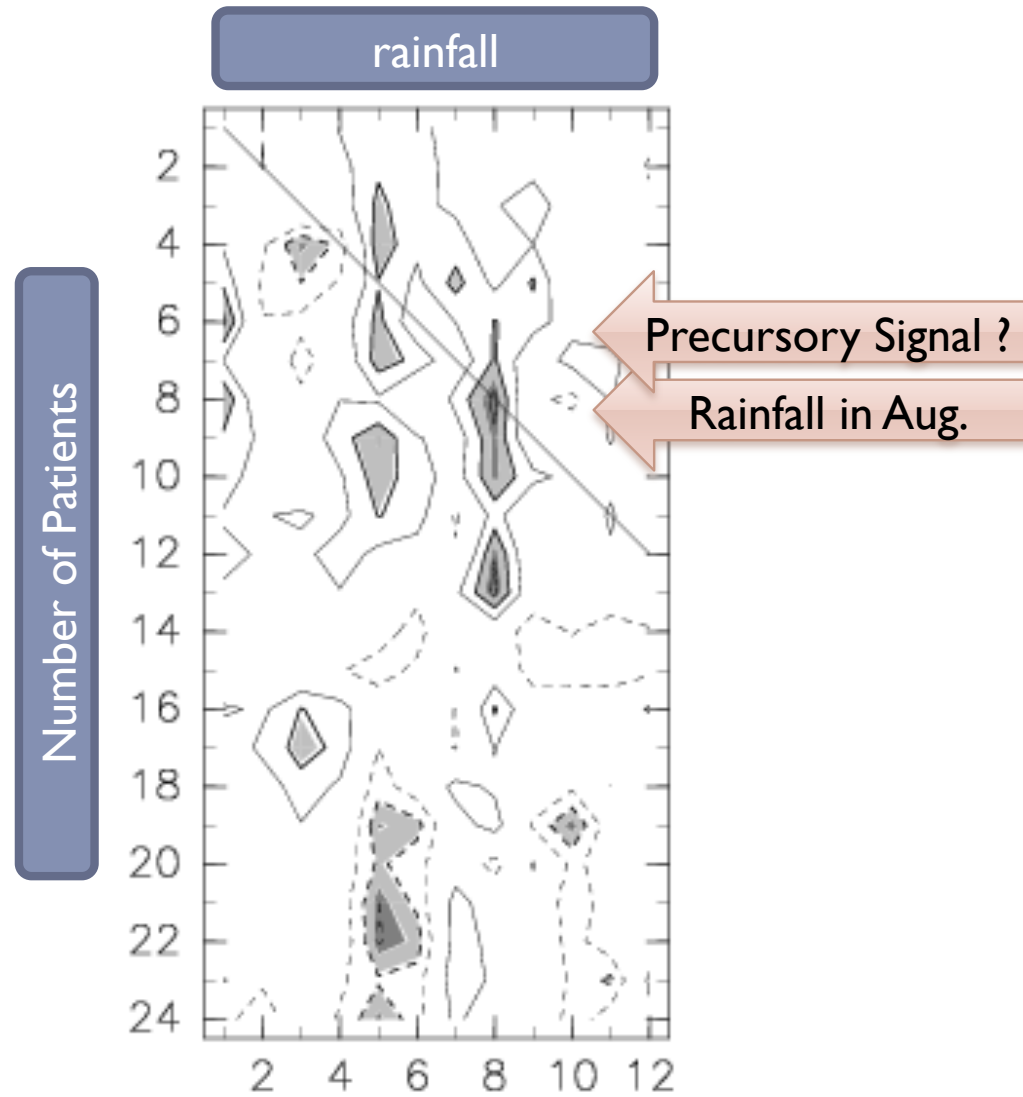
flood

flood

Figure 6: Lower tropospheric (850 hPa) geopotential height anomaly in August

DHAKA上空の西風





CONTOUR INTERVAL = 2.000E-01